Formulation of the Singular Integral Equation Technique for Planar Transmission Lines

ABBAS SAYED OMAR AND KLAUS SCHÜNEMANN, MEMBER, IEEE

Abstract — **The singular integral equation technique is used to determine the normal modes of propagation in general planar transmission lines. Taking finlines as an example, it is demonstrated how high-order modes can effectively and accurately be calculated. It is also shown that complex and backward-wave modes, which are known to exist in rectangular and circular waveguides with dielectric inserts, can also exist in finlines. Besides a discussion of their characteristic features, this paper describes the conditions under which complex and backward-wave modes are found in finlines.**

I. Introduction

PLANAR TRANSMISSION LINES include a variety of structures showing one or more air–dielectric and/or dielectric–dielectric interfaces with metal strips printed at these interfaces. Determining the normal modes of propagation in these structures is of fundamental importance. Due to the completeness property of the set of normal modes [1], an arbitrary electromagnetic field can be expanded within this set so that the problem of determining the field, which can usually be formulated as a solution of integro-differential equations, is reduced to a solution of matrix equations.

Galerkin's method in the spectral domain has been successfully used in analyzing many of these structures (see, e.g., [2]–[4]). In fact, this method is superior over all other known methods if the dominant and the first few higher order modes are computed. A characteristic matrix of order 4 (which corresponds to just two basis functions in the expansion of each of the unknown field components) is quite sufficient to give accurate results. For the determination of still higher order modes, more basis functions are needed so that the order of the characteristic matrix is increased considerably. The singular integral equation technique (SIE), which has been used in [5]–[7] for solving many waveguide problems and in [8] for the analysis of microstrip lines, has the advantage of characterizing the problem by a relatively small-order matrix. Furthermore, it gives accurate results for the high-order modes as will be shown below. Another advantage is that the matrix elements are all given by analytical expressions so that neither infinite sums nor numerical integrations are involved.

Manuscript received March 6, 1985; revised June 26, 1985. This work was supported in part by the Deutsche Forschungsgemeinschaft.

The authors are with the Technische Universität Hamburg-Harburg, Arbeitsbereich Hochfrequenztechnik, Postfach 90 14 03, D-2100 Hamburg 90, West Germany.

Because the weight of the mode in a field expansion series becomes smaller as the mode order goes higher, the determination of the first, say N, modes is the actual need. Determining these N modes without loosing any intermediate ones is actually a problem for planar guiding structures, because it has been found that some pairs of modes become complex modes [9]–[15] within one or more ranges of certain structure parameters (e.g., the slot width in finlines) at a given frequency or, alternatively, within one or more frequency ranges at given structure parameters. This problem will also be investigated here taking the generalized unilateral finline as a case study.

Complex and backward-wave modes are known to exist in circular and rectangular waveguides with dielectric inserts [9]–[17]. It was reported in [9] that the existence of backward-wave modes in a shielded dielectric rod guarantees the existence of complex modes there. More theoretical as well as experimental investigations on complex modes in circular waveguides with dielectric inserts have been performed in [10]–[13]. Although the possibility of backward-wave modes in rectangular waveguides with dielectric inserts has been reported a long time ago [16], [17], complex modes in shielded rectangular dielectric image guides have just been reported [14], [15].

In fact, finlines can be regarded as ridged waveguides with dielectric inserts (the substrate), so that complex and backward-wave modes may also exist there. The nature of such modes in finlines should be similar to that of the corresponding ones in dielectric-loaded rectangular and circular waveguides.

II. Basic Formulation

The electromagnetic field in the generalized unilateral finline shown in Fig. 1 is a linear combination of LSM and LSE parts [1]. These two parts satisfy independently all interface conditions. They are only coupled in order to satisfy the edge conditions, as has been shown in [18]. The tangential electric field $\boldsymbol{E}_t$ and the surface current $\boldsymbol{J}_s$ at the interface $x = 0$ can then be written as

$$\boldsymbol{E}_t = \boldsymbol{E}_t^e + \boldsymbol{E}_t^h \quad \boldsymbol{J}_s = \boldsymbol{J}_s^e + \boldsymbol{J}_s^h$$

where superscripts e and h refer to the LSM and LSE parts, respectively. The LSM part is, however, completely

0018-9480/85/1200-1313$01.00 ©1985 IEEE

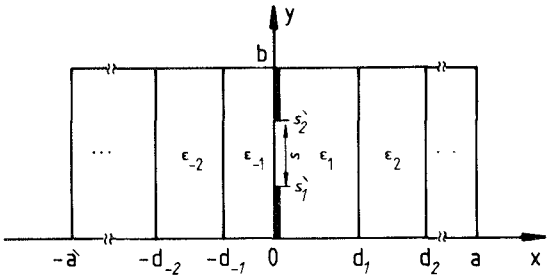

Fig. 1. Generalized unilateral finline.

characterized by the z-components (E_z^e, J_z^e) because

$$E_y^e = (-1/j\beta)\, dE_z^e/dy \quad J_y^e = (-1/j\beta)\, dJ_z^e/dy$$

whereas the LSE part is completely characterized by the y-components (E_y^h, J_y^h) because

$$E_z^h = (1/j\beta)\, dE_y^h/dy \quad J_z^h = (1/j\beta)\, dJ_y^h/dy.$$

With electric walls at $y = 0$ and $y = b$, the four components E_z^e, J_z^e, E_y^h, and J_y^h can be written as

$$E_z^e = \sum_{n=1}^{\infty} A_n^e \sin(n\pi y/b)$$

$$J_z^e = j\omega\epsilon_0 \sum_{n=1}^{\infty} F_n^e A_n^e \sin(n\pi y/b)$$

$$E_y^h = \sum_{n=0}^{\infty} A_n^h \cos(n\pi y/b)$$

$$J_y^h = (1/j\omega\mu_0) \sum_{n=0}^{\infty} F_n^h A_n^h \cos(n\pi y/b) \qquad (1)$$

where F_n^e and F_n^h are the Fourier series expansion coefficients of the LSM and LSE Green's functions, respectively [19]. The SIE technique can now be formulated as follows.

1) Two cosine-series $f_1(y)$ and $f_2(y)$ are constructed in terms of the tangential electric field $\boldsymbol{E}_t$ so that they are unknown only in the slot $(s_1' \leqslant y \leqslant s_2')$. These cosine-series are then given by

$$f_1(y) = \sum_{n=0}^{\infty} A_n^{(1)} \cos(n\pi y/b)$$

$$f_2(y) = \sum_{n=0}^{\infty} A_n^{(2)} \cos(n\pi y/b) \qquad (2)$$

where the coefficients $A_n^{(1)}$ and $A_n^{(2)}$ are, in general, two independent linear combinations of A_n^e and A_n^h.

2) Two sine-series $f_3(y)$ and $f_4(y)$ are constructed in terms of the surface current $\boldsymbol{J}_s$ such that the asymptotic values (as $n \to \infty$) of their coefficients are $A_n^{(1)}$ and $A_n^{(2)}$, respectively. The expansion coefficients of the series $g_1(y)$ and $g_2(y)$ defined by

$$g_1(y) = \sum_{n=1}^{\infty} A_n^{(1)} \sin(n\pi y/b) - f_3(y)$$

$$g_2(y) = \sum_{n=1}^{\infty} A_n^{(2)} \sin(n\pi y/b) - f_4(y) \qquad (3)$$

are then vanishing asymptotically.

3) Applying the boundary conditions to be satisfied by $f_1(y)$ and $f_2(y)$, the coefficients $A_n^{(1)}$ and $A_n^{(2)}$ are determined in terms of integrals of $f_1(y)$ and $f_2(y)$, respectively, taken over the slot $(s_1' \leqslant y \leqslant s_2')$.

4) Substituting these integrals for $A_n^{(1)}$ and $A_n^{(2)}$ into (3) and applying the boundary conditions to be satisfied by $f_3(y)$ and $f_4(y)$, we get two integral equations relating $f_1(y)$ and $f_2(y)$ to $g_1(y)$ and $g_2(y)$, respectively. These integral equations are of the standard singular type. Their solutions are, e.g., given in [7].

5) Due to the asymptotic vanishing of the series coefficients of $g_1(y)$ and $g_2(y)$, these series can be truncated behind the Nth term, so that the functions $f_1(y)$ and $f_2(y)$ are then known in the slot in terms of $A_n^{(1)}$ and $A_n^{(2)}$, $n \leqslant N$.

6) The back substitution of $f_1(y)$ and $f_2(y)$ in the integrals determining $A_n^{(1)}$ and $A_n^{(2)}$, $n \leqslant N$ —step 3) —along with additional conditions (to be discussed later), results in a finite homogeneous system of linear equations, from which the propagation constants, as well as the field expansion coefficients of the different modes, are obtained.

Care should be taken, however, in constructing $(f_1(y), f_2(y))$ and $(f_3(y), f_4(y))$ which are related to $\boldsymbol{E}_t$ and $\boldsymbol{J}_s$, respectively. This is because E_y and J_z, as well as dE_z/dy and dJ_y/dy, are singular at the edges $(y = s_1', y = s_2')$ [20]. The order of singularity is the same for all components, namely $|y - s'|^{-1/2}$. This is exactly the proper type of singularity, which can be described by the SIE technique. Hence, any y-differentiation of either E_y, J_z, dE_z/dy, or dJ_y/dy is not allowed in constructing $f_1(y)$, $f_2(y)$, $f_3(y)$, and $f_4(y)$. This leads to two alternatives. In the first case, $A_n^{(1)}$ and $A_n^{(2)}$ are linear combinations of A_n^e and A_n^h, so that the LSM and LSE parts of the field are coupled from the beginning. We call this formulation the coupling one. In the second case, $A_n^{(1)}$ and $A_n^{(2)}$ are proportional to A_n^e and A_n^h, respectively, so that the LSM and LSE parts of the field are decoupled. Coupling is performed as a final step in the form of additional conditions, as will be shown later. We call this formulation the decoupling one.

A. The Coupling Formulation

The functions $f_1(y)$ and $f_2(y)$ are constructed as

$$f_1(y) = dE_z/dy$$

$$f_2(y) = \left[(k_0^2 - \beta^2)E_y + j\beta(dE_z/dy)\right]/j\omega\mu_0 \qquad (4)$$

whereas $f_3(y)$ and $f_4(y)$ are constructed as

$$f_3(y) = \left[(K^h\beta^2 - K^e k_0^2)J_z + j\beta K^h(dJ_y/dy)\right]/j\omega\epsilon_0 K^e K^h$$

$$f_4(y) = \left[j\beta(K^e - K^h)J_z + K^h(dJ_y/dy)\right]/K^e K^h. \qquad (5)$$

Here K^e and K^h are the asymptotic limits of $(n\pi/b)\cdot F_n^e$ and $F_n^h/(n\pi/b)$, respectively.

The expansion coefficients $A_n^{(1)}$ and $A_n^{(2)}$ of $f_1(y)$ and $f_2(y)$, respectively, are then related to A_n^e and A_n^h by

$$\begin{bmatrix} A_n^{(1)} \\ A_n^{(2)} \end{bmatrix} = \begin{bmatrix} (n\pi/b) & -(n\pi/b)^2/j\beta \\ j\omega\epsilon_0(n\pi/b)/j\beta & \alpha_n^2/j\omega\mu_0 \end{bmatrix} \begin{bmatrix} A_n^e \\ A_n^h \end{bmatrix} \qquad (6)$$

where $\alpha_n^2 = k_0^2 - \beta^2 - (n\pi/b)^2$. The series expansions of $f_3(y)$ and $f_4(y)$ are readily proved to have the following forms:

$$f_3(y) = \sum_{n=1}^{\infty} \left[P_n^{(1)}A_n^{(1)} + P_n^{(2)}A_n^{(2)}\right] \sin(n\pi y/b)$$

$$f_4(y) = \sum_{n=1}^{\infty} \left[Q_n^{(1)}A_n^{(1)} + Q_n^{(2)}A_n^{(2)}\right] \sin(n\pi y/b) \quad (7)$$

where $P_n^{(1)}$, $P_n^{(2)}$, $Q_n^{(1)}$, and $Q_n^{(2)}$ are given in terms of F_n^e and F_n^h with their asymptotic limits being 1, 0, 0, and 1, respectively.

The series $g_1(y)$ and $g_2(y)$ defined in (3) are then given by

$$g_1(y) = \sum_{n=1}^{\infty} \left[(1 - P_n^{(1)})A_n^{(1)} - P_n^{(2)}A_n^{(2)}\right] \sin(n\pi y/b)$$

$$g_2(y) = \sum_{n=1}^{\infty} \left[-Q_n^{(1)}A_n^{(1)} + (1 - Q_n^{(2)})A_n^{(2)}\right] \sin(n\pi y/b). \quad (8)$$

Defining

$$\varphi = \pi y/b, \quad \varphi_1 = \pi s_1'/b, \quad \varphi_2 = \pi s_2'/b \quad (9)$$

we can write for the boundary conditions to be imposed on $f_1(\varphi), \cdots, f_4(\varphi)$

$$f_i(\varphi) = \begin{cases} 0 & (0 \leqslant \varphi \leqslant \varphi_1,\ \varphi_2 \leqslant \varphi \leqslant \pi) \\ h_i(\varphi) & (\varphi_1 \leqslant \varphi \leqslant \varphi_2) \end{cases}$$

$$f_{i+2}(\varphi) = 0 \qquad (\varphi_1 \leqslant \varphi \leqslant \varphi_2), \quad i = 1,2. \quad (10)$$

The coefficients $A_n^{(1)}$ and $A_n^{(2)}$ are then given by

$$A_0^{(i)} = [(i-1)/\pi] \int_{\varphi_1}^{\varphi_2} h_i(\varphi)\, d\varphi$$

$$A_n^{(i)} = [2/\pi] \int_{\varphi_1}^{\varphi_2} h_i(\varphi) \cos n\varphi\, d\varphi, \qquad i = 1,2. \quad (11)$$

Making use of the transformations

$$\cos\varphi = \cos[(\varphi_2 + \varphi_1)/2] \cos[(\varphi_2 - \varphi_1)/2] - \eta \sin[(\varphi_2 + \varphi_1)/2] \sin[(\varphi_2 - \varphi_1)/2]$$

$$G_i(\eta) = g_i(\varphi)/\sin\varphi$$

$$H_i(\eta) = h_i(\varphi)/\sin\varphi, \qquad i = 1,2 \quad (12)$$

we get the following standard singular integral equations:

$$G_i(\eta) = (1/\pi) \int_{-1}^{+1} H_i(\eta')/(\eta - \eta')\, d\eta', \qquad -1 \leqslant \eta \leqslant +1, \quad i = 1,2. \quad (13)$$

Their solutions are

$$H_i(\eta) = (1-\eta^2)^{-1/2} \left[A_0^{(i)}/\sin[(\varphi_2 + \varphi_1)/2] \cdot \sin[(\varphi_2 - \varphi_1)/2] + (1/\pi) \int_{-1}^{+1} (1-\eta'^2)^{1/2} \cdot G_i(\eta')/(\eta' - \eta)\, d\eta', \qquad i = 1,2. \quad (14)$$

As may easily be seen, the vanishing of $f_1(y)$ and $f_2(y)$ on the metal fins and that of $f_3(y)$ and $f_4(y)$ in the slot, which are the considered boundary conditions, are only necessary conditions for the vanishing of $\boldsymbol{E}_t$ and $\boldsymbol{J}_s$ on their respective regions (i.e., $\boldsymbol{E}_t$ on the fins and $\boldsymbol{J}_s$ in the slot). This guarantees the vanishing of E_y and J_z on their respective regions but only the constancy of E_z and J_y on their respective regions. However, points $y = 0$ and $y = b$, at which $E_z = 0$, belong to the fins, so that the constant value of E_z on the fins is automatically zero. Hence, just one additional condition must be imposed, namely the vanishing of J_y at any point in the slot, so that the constant value of J_y over the slot is put to zero.

B. The Decoupling Formulation

Functions $f_1(y)$ and $f_2(y)$ are now constructed as

$$df_1/dy = \nabla_t \cdot \boldsymbol{E}_t = -\Delta_t E_z^e/j\beta$$

$$f_2(y) = \hat{\boldsymbol{i}} \cdot (\nabla_t \times \boldsymbol{E}_t) = \Delta_t E_y^h/j\beta \quad (15)$$

whereas functions $f_3(y)$ and $f_4(y)$ are constructed according to

$$f_3(y) = -(\nabla_t \cdot \boldsymbol{J}_s)/j\omega\epsilon_0 K^e = -\Delta_t J_z^e/\omega\epsilon_0 \beta K^e$$

$$df_4/dy = j\omega\mu_0 [\hat{\boldsymbol{i}} \cdot (\nabla_t \times \boldsymbol{J}_s)]/K^h = \omega\mu_0 \Delta_t J_y^h/\beta K^h. \quad (16)$$

Here ∇_t and Δ_t are the del and laplacian operators in the y–z-plane, respectively, and $\hat{\boldsymbol{i}}$ is the unit vector in the x-directions. The boundary conditions to be imposed on $f_1(y)$, $f_2(y)$, $f_3(y)$, and $f_4(y)$ (which are $df_1/dy = 0 = f_2(y)$ on the fins and $f_3(y) = 0 = df_4/dy$ in the slot) are again necessary conditions for the vanishing of $\boldsymbol{E}_t$ and $\boldsymbol{J}_s$ on their respective regions. In this case, it is guaranteed that the individual components of $\boldsymbol{E}_t$ and $\boldsymbol{J}_s$ are harmonic functions on their respective regions [19], so that additional conditions must be imposed. These conditions can be shown to be the vanishing of only one component of $\boldsymbol{E}_t$ and $\boldsymbol{J}_s$ on the boundaries of their respective regions, which are the edges ($y = s_1'$, $y = s_2'$).

III. High-Order Modes Accuracy

The only approximation involved in the SIE technique is the truncation of the infinite series $g_1(y)$ and $g_2(y)$ behind the Nth term. However, it can be proved that the nth coefficients of $g_1(y)$ and $g_2(y)$ are almost zero if $(n\pi/b)^2 > (\hat{\epsilon}_r k_0^2 - \beta^2)$, where $\hat{\epsilon}_r$ is the largest dielectric constant involved. This limits the number of high-order modes, which can be calculated accurately, because the propagation constant of the highest order mode (which usually is evanescent) should satisfy

$$|\beta|^2 < [(N+1)\pi/b]^2 - \hat{\epsilon}_r k_0^2.$$

For normally used dimensions, dielectric constants, and operation frequencies, $N = 3$ (corresponding to a characteristic matrix of order 7) is sufficient to give the first 30 modes accurately.

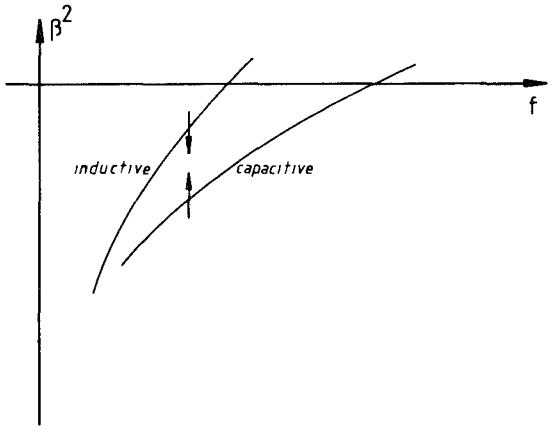

Fig. 2. Typical behavior of inductive and capacitive modes with increasing slot width.

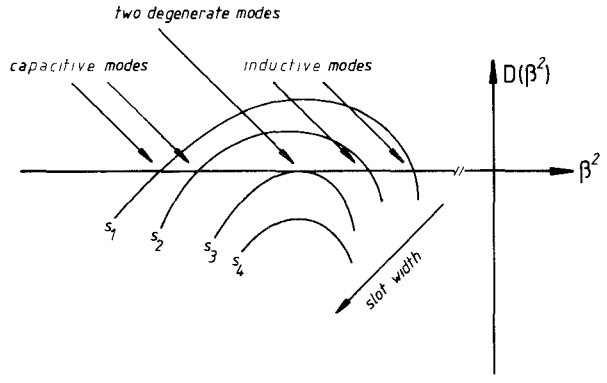

Fig. 3. Typical behavior of how two modes disappear.

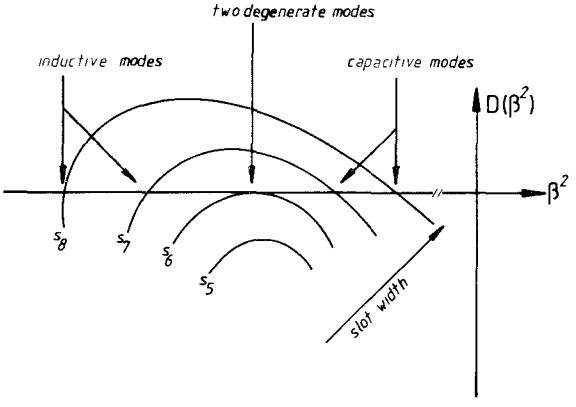

Fig. 4. Typical behavior of how two modes reappear

IV. The Problem of Mode Disappearance

It has been shown in [18], that the modes of the generalized unilateral finline behave either inductively or capacitively if they are below cutoff. The interesting difference between the two types is the dependence of their propagation constants on the slot width. The propagation constant squared (β^2) (which is always a real number in the lossless case, whether the mode is below or above cutoff) of an inductive (a capacitive) mode decreases (increases) versus the slot width, as is shown in Fig. 2. Consider now the modes for a certain slot width being arranged according to their β^2. If one of any two successive modes is inductive with β_i^2 while the other is capacitive with a smaller β_c^2, and the slot width is increased, then β_i^2 and β_c^2 approach each other up to a certain slot width where $\beta_i^2 = \beta_c^2$. For this slot width, we get two degenerate modes which are no longer orthogonal. They should be treated carefully because of the strong coupling between them. If the slot width is increased beyond this value both modes will disappear. This will be illustrated in the following.

The final step in nearly all mode analysis methods is the solution of a homogeneous system of linear equations which can be written as a matrix equation

$$[C]\cdot \boldsymbol{X} = 0.$$

The elements of the matrix $[C]$, usually called the characteristic matrix, depend on the unknown propagation constant β. The elements of the column vector $\boldsymbol{X}$ determine the electromagnetic-field configuration of the mode whose propagation constant is β. The elements of $[C]$ can always be normalized in such a way that they are all real functions of β^2 if the structure is lossless. The matrix equation is solved by looking for the values of β, making the matrix $[C]$ singular. Each of these values characterizes one of the structure modes.

For our case, we assume that the finline is lossless so that the determinant of the matrix $[C]$ is a real function $D(\beta^2)$. The different modes are then obtained by looking for the zeros of $D(\beta^2)$. The behavior of $D(\beta^2)$ near the aforementioned successive inductive and capacitive modes for a certain range of the slot width typically is as shown in Fig. 3. As the slot width increases from s_1 to s_2, β^2 of the inductive mode decreases, while that of the capacitive mode increases. At s_3 the two modes become degenerate and at s_4 they disappear completely. This effect occurs within a certain range of slot widths. Afterwards, we get the situation shown in Fig. 4. At s_5 ($> s_4$), the two modes are still nonexisting; at s_6, two degenerate modes are obtained, and for $s > s_6$, two nondegenerate modes exist again: one is inductive (now to the left-hand side) and the other is capacitive (to the right-hand side). It is important to note that when the slot width increases from s_7 to s_8, β^2 of the inductive mode still decreases while that of the capacitive mode still increases.

The disappearance of some modes at a given frequency within a range of slot widths (namely for $s_3 < s < s_6$) or, alternatively, at a given slot width within a range of frequencies is physically impossible. This can be explained by regarding the finline discontinuity shown in Fig. 5. Assuming that $\delta s \ll s_3$, this discontinuity is very weak, so that any incident mode in finline "a" can be nearly matched at z_0 to a single mode in finline "b" of nearly the same field configuration (whose propagation constant is very near that of the incident mode). Let us hypothetically assume that the incident field in finline "a" consists only of the two degenerate modes (shown in Fig. 3). If there were no modes in finline "b" with propagation constants

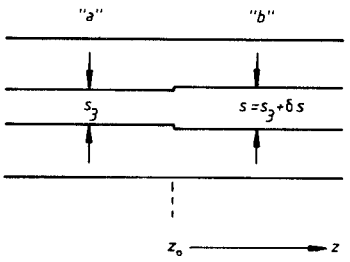

Fig. 5. A weak finline discontinuity.

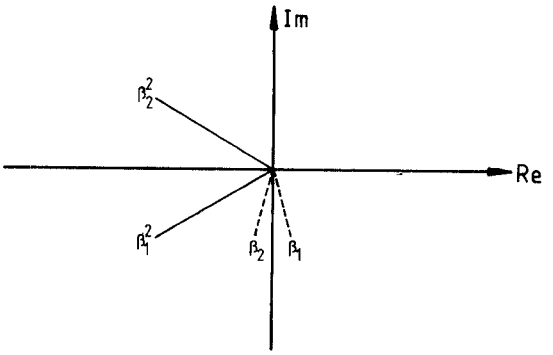

Fig. 6. The propagation constants of two complex modes.

which are near to that of the incident modes in finline "a", we should expect that there are also no modes in finline "b" with field configurations which are similar to those of the incident modes in finline "a". This means that the matching at z_0 requires a large number of excited modes at both sides of discontinuity, which contradicts with the weakness of the discontinuity.

V. Finline Complex Modes

Modes with complex propagation constants in lossless guiding structures have been known for a long time as "complex modes" [9]. They have been reported in [9] to occur as a continuation of backward-wave modes in the modal spectrum of shielded dielectric rods. They can also exist even if there is no region of the spectrum in which backward-wave modes can propagate [10]. The same has been reported in [14] and [15] with respect to shielded rectangular dielectric image guides. In both cases, backward-wave and complex modes can exist in a waveguide with a dielectric insert as modes of "hybrid-type." They cannot exist in a dielectric loaded circular waveguide without azimuthal dependence, because modes with no azimuthal dependence are either TE-type or TM-type modes. They can also not exist in the dielectric slab loaded rectangular waveguide because the modes of this structure are either of the LSE type or LSM type [1].

Finlines are, in fact, dielectric-loaded ridged waveguides, the modes of which are all of hybrid-type. Complex and backward-wave modes are consequently possible in finlines.

Now, we return to the problem of mode disappearance. The only possibility for the disappearance of the aforementioned two modes is that their β^2 are no longer real. Hence, zeros of $D(\beta^2)$ must be looked for in the complex plane rather than on the real axis. Although $D(\beta^2)$ is a complicated function and not at all a "polynomial with real coefficients," its zeros for the particular slot width range are found to be always a complex conjugate pair.

Now, let us investigate a pair of complex modes in some details. As shown in Fig. 6, let the corresponding complex conjugate zeros of $D(\beta^2)$ be β_1^2 and β_2^2. Their square roots, which are physically possible for a z-dependence $e^{-j\beta z}$ and a time dependence $e^{j\omega t}$, are also shown and can be written as

$$\beta_1 = \beta' - j\alpha' \quad \beta_2 = -\beta' - j\alpha'$$

where α' and β' are positive numbers. This means that one mode propagates in the $+z$-direction and is attenuated in the same direction. The other mode is also attenuated in this direction; it propagates, however, in the $-z$-direction. From the first view, it is easily stated that a mode with the complex propagation constant β_1 propagates in the same direction, in which it is attenuated; this means a continuous energy loss, although the structure has been assumed lossless. The other mode with propagation constant β_2 propagates opposite to the direction in which it is damped; this means a continuous energy gain, although the structure is passive. This point of view would be correct only if the two modes were not coupled. In fact, it has been found as a result of extensive numerical investigations that the two modes are so strongly coupled, that the electric field of each mode does not couple to its own magnetic field, but to the magnetic field of the other mode, i.e.,

$$\int_S (\boldsymbol{e}_1 \times \boldsymbol{h}_1^*)\cdot d\boldsymbol{S} = 0 = \int_S (\boldsymbol{e}_2 \times \boldsymbol{h}_2^*)\cdot d\boldsymbol{S} \tag{17}$$

$$\int_S (\boldsymbol{e}_1 \times \boldsymbol{h}_2^*)\cdot d\boldsymbol{S} = p \neq 0 \quad \int_S (\boldsymbol{e}_2 \times \boldsymbol{h}_1^*)\cdot d\boldsymbol{S} = -p^*. \tag{18}$$

Here $\boldsymbol{e}_1(\boldsymbol{h}_1)$ and $\boldsymbol{e}_2(\boldsymbol{h}_2)$ are the transverse electric- (magnetic-) field vectors of the modes with propagation constants β_1 and β_2, respectively, and S is the finline cross section. It has also been found from the same numerical investigations that, although the two modes are coupled in energy sense, they are still orthogonal in the sense of the following orthogonality relations:

$$\int_S (\boldsymbol{e}_1 \times \boldsymbol{h}_2)\cdot d\boldsymbol{S} = 0 = \int_S (\boldsymbol{e}_2 \times \boldsymbol{h}_1)\cdot d\boldsymbol{S} \tag{19}$$

$$\int_S (\boldsymbol{e}_1 \times \boldsymbol{h}_1)\cdot d\boldsymbol{S} = p \quad \int_S (\boldsymbol{e}_2 \times \boldsymbol{h}_2)\cdot d\boldsymbol{S} = -p^*. \tag{20}$$

A similar result has also been obtained for the shielded dielectric rod [13] and the shielded rectangular dielectric image guide [15]. Equations (17) and (18) mean that each mode cannot exist alone; both should always exist together, if they exist. As will be shown below, (18) plays an important role in the evanescent nature of the two coupled modes.

Now we investigate the problem from the energy point of view. Let us assume that the two questionable modes are

excited (by, e.g., a certain discontinuity). Because each of these modes is not coupled to the other modes which may also be excited, it is sufficient to study the energy contained in these two modes only. Let $\boldsymbol{E}$ and $\boldsymbol{H}$ be the transverse electric- and magnetic-field vectors, respectively, of the two superposed modes; i.e., let

$$\boldsymbol{E} = A_1 e^{-j\beta_1 z}\boldsymbol{e}_1 + A_2 e^{-j\beta_2 z}\boldsymbol{e}_2$$

$$\boldsymbol{H} = A_1 e^{-j\beta_1 z}\boldsymbol{h}_1 + A_2 e^{-j\beta_2 z}\boldsymbol{h}_2.$$

Integrating the Poynting vector over the finline cross section, and making use of (17) and (18), one obtains

$$P = \int_S (\boldsymbol{E} \times \boldsymbol{H}^*)\cdot d\boldsymbol{S} = jW \sin(2\beta' z + \vartheta) e^{-2\alpha' z}$$

where $A_1 A_2^* p = -(W/2)e^{-j\vartheta}$. The vanishing of the real part of P guarantees that the two superposed modes carry no active power, i.e., they behave as a whole evanescently. The energy stored in these superposed modes is shown in Fig. 7. It oscillates along the line once being inductive and once being capacitive in nature with exponential decay. This behavior is not, however, unexpected because one of these two modes was inductive and the other one was capacitive before their β^2 disappeared on the real axis.

The vanishing of the active power transmitted by a pair of complex modes has also been reported in [13] and [15] for the shielded dielectric rod and image guide, respectively, although using a different reasoning, namely, the total active powers transmitted inside and outside the dielectric region, are of equal magnitudes but of opposite directions.

VI. Backward-Wave Modes in Finlines

Although pairs of complex modes can exist in finlines for any value of the substrate dielectric constant ϵ_r, backward-wave modes can only exist when the value of ϵ_r is relatively high. Small values of ϵ_r, which are usually used for normal finlines (typically, $\epsilon_r = 2.22$), lead to a very small (β'/α') ratio of any pair of complex modes which can exist. No backward-wave modes have been found for small values of ϵ_r. However, if both ϵ_r and the substrate thickness are considerably increased, the (β'/α') ratio of low-order complex modes increases considerably. In addition, if a pair of complex modes is near cutoff, it may be continued into a pair of forward- and backward-wave modes.

Finally, we would like to state that, although finlines have only been investigated, we believe that complex and backward-wave modes can also exist in any planar guiding structure with closed conducting boundaries.

VII. Numerical Results

To illustrate the fast convergence of truncating the characteristic matrix, the propagation constants of the first 30 modes of a unilateral finline have been calculated for three different slot widths using a matrix order of 5, 7, and 9 (i.e., truncating the infinite series $g_1(y)$ and $g_2(y)$ behind the 2nd, 3rd, and 4th term, respectively. The results in Tables I, II, and III show that, whatever the slot width, a matrix order of 7 is quite sufficient to give accurate results for the first 30 modes.

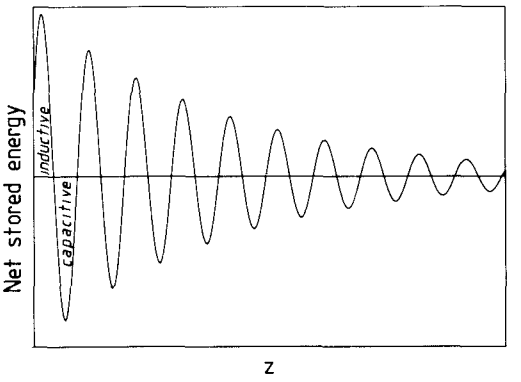

Fig. 7. Net stored energy of the superposed complex modes.

The four coupling integrals given in (17) and (18) have been numerically calculated by using a 100-term Fourier expansion for each field component. The results are tabulated in Table IV for the slot width ranging between 0.5 mm and 1.5 mm. For 0.5 mm $\leqslant s \leqslant$ 0.7 mm, we have two ordinary evanescent modes. The first (second) is inductive (capacitive) with β^2 decreasing (increasing) versus s. The values of the coupling integrals are in good agreement to the exact values given, e.g, in [1] for general inhomogeneously filled waveguides. For 0.8 mm $\leqslant s \leqslant$ 1.3 mm, we have a pair of complex modes. The coupling integrals are again in good agreement with the values given by (17) and (18). The smallness of the (β'/α') ratio is due to the smallness of the substrate dielectric constant $(\epsilon_r = 2.22)$ and the substrate thickness. Higher (β'/α') values can be obtained by increasing these parameters as will be shown later. Finally, for 1.4 mm $\leqslant s \leqslant$ 1.5 mm, we have two ordinary evanescent modes again. The first (second) is now capacitive (inductive) with β^2 increasing (decreasing) versus s. The quantitative values of the coupling integrals are again in good agreement to the exact values given in [1].

The frequency dependencies of β' and α' of the complex modes existing in the same finline with a slot width of 1.0 mm are plotted in Fig. 8. For $F < 15$ GHz, we have two ordinary evanescent modes. Their dispersion curves are not distinugishable in the figure. The values of their α' at, e.g., $F = 10$ GHz are (3.1608 mm^{-1}) and (3.1673 mm^{-1}). For 15 GHz $\leqslant F \leqslant$ 117 GHz, we have a pair of complex modes. An interesting observation is the wideness of the frequency band over which the complex modes exist (more than 100 GHz). This wideness is, however, related to the smallness of the (β'/α') ratio (note that the upper plot of Fig. 8 is for 100 times β', whereas the lower one is for α') because this band decreases considerably when the (β'/α') ratio increases as will be shown below. For $F \geqslant 118$ GHz, the two complex modes are continued into two ordinary evanescent modes again.

Complex modes in a finline with a high value of the substrate dielectric constant $(\epsilon_r = 20)$ and a relatively thick

TABLE I
THE PROPAGATION CONSTANTS OF THE FIRST 30 MODES IN A UNILATERAL FINLINE OF 0.2-mm SLOT WIDTH

mode no. / matrix order	1	2	3	4	5	6	7	8	9	10
5 x 5	+0.6837	-j 0.6067	-j 0.7448	-j 1.5955	-j 1.6489	-j 1.6801	-j 1.7472	-j 1.9938	-j 2.4747	-j 2.5509
7 x 7	+0.6824	-j 0.6067	-j 0.7448	-j 1.5955	-j 1.6489	-j 1.6801	-j 1.7470	-j 1.9926	-j 2.4747	-j 2.5495
9 x 9	+0.6820	-j 0.6067	-j 0.7448	-j 1.5955	-j 1.6489	-j 1.6800	-j 1.7470	-j 1.9922	-j 2.4747	-j 2.5491

mode no. / matrix order	11	12	13	14	15	16	17	18	19	20
5 x 5	-j 2.7083	-j 3.0745	-j 3.1136	-j 3.2065	-j 3.2384	-j 3.3653	-j 3.4763	-j 3.4976	-j 3.6058	-j 3.6683
7 x 7	-j 2.7073	-j 3.0738	-j 3.1136	-j 3.2065	-j 3.2375	-j 3.3649	-j 3.4763	-j 3.4971	-j 3.6057	-j 3.6656
9 x 9	-j 2.7070	-j 3.0735	-j 3.1136	-j 3.2065	-j 3.2372	-j 3.3648	-j 3.4763	-j 3.4969	-j 3.6057	-j 3.6648

mode no. / matrix order	21	22	23	24	25	26	27	28	29	30
5 x 5	-j 3.8140	-j 3.8787	-j 3.9308	-j 3.9683	-j 4.0196	-j 4.0854	-j 4.2335	-j 4.3530	-j 4.3621	-j 4.4326
7 x 7	-j 3.8130	-j 3.8787	-j 3.9308	-j 3.9663	-j 4.0196	-j 4.0786	-j 4.2318	-j 4.3483	-j 4.3635	-j 4.4326
9 x 9	-j 3.8127	-j 3.8787	-j 3.9308	-j 3.9658	-j 4.0196	-j 4.0770	-j 4.2314	-j 4.3475	-j 4.3637	-j 4.4326

Parameters: $a = 2$ $b = 3.556$ mm, substrate thickness = 0.254 mm, substrate dielectric constant = 2.22, frequency = 30 GHz.

TABLE II
THE PROPAGATION CONSTANTS OF THE FIRST 30 MODES IN A UNILATERAL FINLINE OF 1.0-mm SLOT WIDTH

mode no. / matrix order	1	2	3	4	5	6	7	8	9	10
5 x 5	+0.5976	-j 0.6154	-j 0.8564	-j 1.6031	-j 1.6489	-j 1.6847	-j 1.7697	-j 1.8877	-j 2.0873	-j 2.4642
7 x 7	+0.5976	-j 0.6154	-j 0.8564	-j 1.6031	-j 1.6489	-j 1.6847	-j 1.7697	-j 1.8877	-j 2.0873	-j 2.4640
9 x 9	+0.5975	-j 0.6154	-j 0.8563	-j 1.6031	-j 1.6489	-j 1.6847	-j 1.7696	-j 1.8877	-j 2.0872	-j 2.4640

mode no. / matrix order	11	12	13	14	15	16	17	18	19	20
5 x 5	-j 2.4754	-j 2.6055	-j 2.8094	-j 3.2019	-j 3.2757	-j 3.4238	-j 3.4764	-j 3.5024	-j 3.5950	-j 3.6260
7 x 7	-j 2.4754	-j 2.6054	-j 2.8094	-j 3.2014	-j 3.2757	-j 3.4230	-j 3.4764	-j 3.5021	-j 3.5948	-j 3.6234
9 x 9	-j 2.4754	-j 2.6054	-j 2.8089	-j 3.2012	-j 3.2756	-j 3.4221	-j 3.4764	-j 3.5021	-j 3.5947	-j 3.6225

mode no. / matrix order	21	22	23	24	25	26	27	28	29	30
5 x 5	-j 3.6920	-j 3.8520	-j 3.8605	-j 3.9270	-j 3.9783	-j 4.0130	-j 4.1337	-j 4.2822	-j 4.4232	-j 4.4794
7 x 7	-j 3.6916	-j 3.8518	-j 3.8563	-j 3.9265	-j 3.9750	-j 4.0120	-j 4.1326	-j 4.2815	-j 4.4212	-j 4.4729
9 x 9	-j 3.6916	-j 3.8516	-j 3.8540	-j 3.9263	-j 3.9746	-j 4.0115	-j 4.1326	-j 4.2806	-j 4.3498	-j 4.3543

Parameters: As in Table I.

TABLE III
THE PROPAGATION CONSTANTS OF THE FIRST 30 MODES IN A UNILATERAL FINLINE OF 3.0-mm SLOT WIDTH

mode no. / matrix order	1	2	3	4	5	6	7	8	9	10
5 x 5	+0.4931	-j 0.6207	-j 1.1356	-j 1.6489	-j 1.6501	-j 1.7080	-j 1.7391	-j 1.8721	-j 1.8777	-j 2.0731
7 x 7	+0.4930	-j 0.6207	-j 1.1356	-j 1.6489	-j 1.6501	-j 1.7080	-j 1.7382	-j 1.8721	-j 1.8776	-j 2.0723
9 x 9	+0.4930	-j 0.6207	-j 1.1355	-j 1.6489	-j 1.6501	-j 1.7080	-j 1.7379	-j 1.8721	-j 1.8776	-j 2.0719

mode no. / matrix order	11	12	13	14	15	16	17	18	19	20
5 x 5	-j 2.4167	-j 2.4415	-j 2.5705	-j 2.9917	-j 3.1180	-j 3.1648	-j 3.4764	-j 3.4816	-j 3.5054	-j 3.5621
7 x 7	-j 2.4166	-j 2.4415	-j 2.5703	-j 2.9903	-j 3.1178	-j 3.1647	-j 3.4764	-j 3.4815	-j 3.5054	-j 3.5584
9 x 9	-j 2.4166	-j 2.4414	-j 2.5702	-j 2.9897	-j 3.1177	-j 3.1647	-j 3.4764	-j 3.4814	-j 3.5054	-j 3.5573

mode no. / matrix order	21	22	23	24	25	26	27	28	29	30
5 x 5	-j 3.5867	-j 3.5914	-j 3.7128	-j 3.7903	-j 3.8597	-j 3.9001	-j 3.9082	-j 3.9162	-j 3.9609	-j 4.0982
7 x 7	-j 3.5868	-j 3.5913	-j 3.7121	-j 3.7793	-j 3.8555	-j 3.9002	-j 3.9080	-j 3.9160	-j 3.9607	-j 4.0964
9 x 9	-j 3.5869	-j 3.5913	-j 3.7118	-j 3.7762	-j 3.8534	-j 3.9002	-j 3.9079	-j 3.9159	-j 3.9607	-j 4.0953

Parameters: As in Table I.

TABLE IV
THE COUPLING INTEGRALS ($I_{ij} = \int_S (\boldsymbol{e}_i \times \boldsymbol{h}_j^*) \cdot d\boldsymbol{S}$) BETWEEN TWO MODES OF A UNILATERAL FINLINE

slot width (m.m.)	0.5	0.7	0.8	1.0
β_1	(0.00000)-j(3.08835)	(0.00000)-j(3.09792)	+(0.00368)-j(3.10463)	+(0.00855)-j(3.10558)
β_2	(0.00000)-j(3.11208)	(0.00000)-j(3.10892)	-(0.00368)-j(3.10463)	-(0.00855)-j(3.10558)
I_{11}	(0.00000)+j(1.00000)	(0.00000)+j(1.00000)	+(0.00009)+j(0.00012)	-(0.00023)+j(0.00017)
I_{12}	(0.00000)+j(0.00038)	(0.00000)+j(0.00024)	+(0.90786)+j(0.41927)	+(0.28358)+j(0.95895)
I_{21}	(0.00000)+j(0.00011)	(0.00000)-j(0.00007)	-(0.90786)+j(0.41927)	-(0.28358)+j(0.95895)
I_{22}	(0.00000)-j(1.00000)	(0.00000)-j(1.00000)	-(0.00009)+j(0.00012)	+(0.00023)+j(0.00017)

slot width (m.m.)	1.1	1.3	1.4	1.5
β_1	+(0.00912)-j(3.10489)	+(0.00192)-j(3.09950)	(0.00000)-j(3.08082)	(0.00000)-j(3.06148)
β_2	-(0.00912)-j(3.10489)	-(0.00192)-j(3.09950)	(0.00000)-j(3.10667)	(0.00000)-j(3.10869)
I_{11}	-(0.00048)+j(0.00011)	-(0.00102)-j(0.00369)	(0.00000)-j(1.00000)	(0.00000)-j(1.00000)
I_{12}	-(0.08344)+j(0.99651)	-(0.98287)+j(0.18427)	(0.00000)-j(0.00251)	(0.00000)-j(0.00259)
I_{21}	+(0.08344)+j(0.99651)	+(0.98287)+j(0.18427)	(0.00000)-j(0.00003)	(0.00000)+j(0.00010)
I_{22}	+(0.00048)+j(0.00011)	+(0.00102)-j(0.00369)	(0.00000)+j(1.00000)	(0.00000)+j(1.00000)

Parameters: As in Table I.

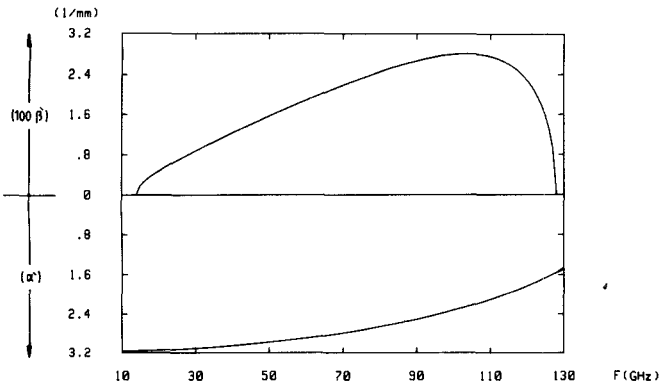

Fig. 8. Dispersion characteristics of a pair of complex modes in a unilateral finline. Parameters: $a = 2$ $b = 3.556$ mm, substrate thickness = 0.254 mm, substrate dielectric constant = 2.22, slot width = 1.0 mm.

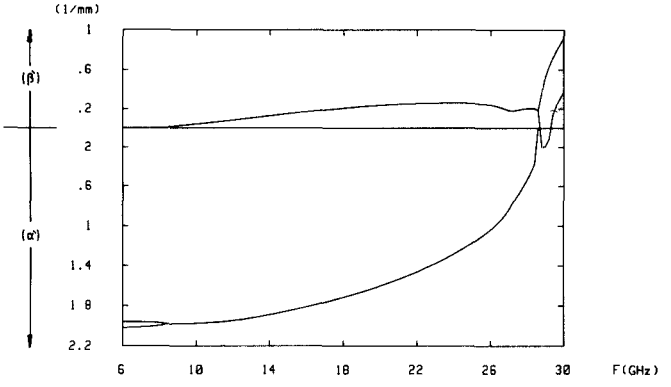

Fig. 9. Dispersion characteristics of a pair of complex modes in a unilateral finline. Parameters: $a = 2$ $b = 3.556$ mm, substrate thickness = 1.067 mm, substrate dielectric constant = 20, slot width = 0.4 mm.

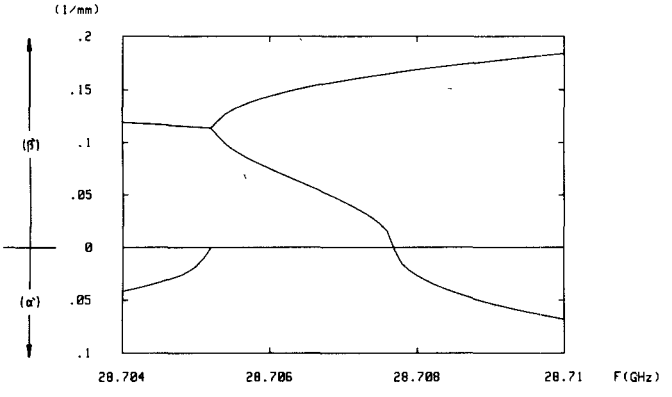

Fig. 10. Dispersion characteristics of a pair of forward- and backward-wave modes in a unilateral finline. Parameters: As in Fig. 9.

substrate (0.3 times the housing height) are finally investigated. The dispersion curves of β' and α' are plotted in Fig. 9. The (β'/α') ratio is much larger than in the previous case, whereas the frequency band over which the complex modes exist is much smaller now (about 20 GHz). The complex modes in this case are continued into a pair of forward- and backward-wave modes. The backward-wave mode exists over an extremely narrow frequency band. This is shown in more detail in Fig. 10.

Acknowledgment

The authors thank C. Bühst for preparing the manuscript, and E. Jensen for helpful discussions.

References

[1] R. E. Collin, *Field Theory of Guided Waves. New York: McGraw-Hill*, 1960.

[2] J. B. Davies and D.M.-Syahkal,"Spectral domain solution of arbitrary coplanar transmission line with multilayer substrate," *IEEE Trans. Microwave Theory Tech.*, vol. MTT-25, pp. 143–146, 1977.

[3] L.-P. Schmidt and T. Itoh, "Spectral domain analysis of dominant and higher order modes in fin-lines," *IEEE Trans. Microwave Theory Tech.*, vol. MTT-28, pp. 981–985, 1980.

[4] L.-P. Schmidt, T. Itoh, and H. Hofmann, "Characteristic of unilateral fin-line structures with arbitrary located slots," *IEEE Trans. Microwave Theory Tech.*, vol. MTT-29, pp. 352–355, 1981.

[5] L. Lewin, *Advanced Theory of Waveguides*. London: Iliffe, 1951.

[6] L. Lewin, "The use of singular integral equations in the solution of waveguide problems," in *Advances of Microwaves*, vol. 1, Leo Young, Ed. New York: Academic Press, 1966.

[7] L. Lewin, *Theory of Waveguides*. London: Newnes Butterworths, 1975.

[8] R. Mittra and T. Itoh, "A new technique for the analysis of the dispersion characteristics of microstrip lines," *IEEE Trans. Microwave Theory Tech.*, vol. MTT-19, pp. 47–56, 1971.

[9] P. J. B. Clarricoats and B. C. Taylor, "Evanescent and propagating modes of dielectric-loaded circular waveguide," *Proc. Inst. Elec. Eng.*, vol. 111, pp. 1951–1956, 1964.

[10] P. J. B. Clarricoats and K. R. Slinn, "Complex modes of propagation in dielectric loaded circular waveguides," *Electron Lett.*, vol. 1, pp. 145–146, 1965.

[11] S. B. Rayevskiy, "Some properties of complex waves in a double-layer circular, shielded waveguides," *Radio Eng. Electron Phys.*, vol. 21, pp. 36–39, 1976.

[12] V. A. Kalmyk, S. B. Rayevskiy, and V. P. Ygryumov, "An experimental verification of existence of complex waves in a two-layer, circular, shielded, waveguide," *Radio Eng. Electron Phys.*, vol. 23, pp. 16–19, 1978.

[13] H. Katzier and F. J. K. Lange, "Grundlegende Eigenschaften komplexer Wellen am Beispiel der geschirmten kreiszylindrischen dielektrischen Leitung," *Arch. Elek. Übertragung.*, vol. AEÜ-37, pp. 1–5, 1983.

[14] U. Crombach, "Complex waves on shielded lossless rectangular dielectric image guide," *Electron Lett.*, vol. 19, pp. 557–558, 1983.

[15] J. Strube and F. Arndt, "Rigorous hybrid-mode analysis of the transition from rectangular waveguide to shielded dielectric image guide," *IEEE Trans. Microwave Theory Tech.*, vol. MTT-33, pp. 391–401, 1985.

[16] A. Lavik and H.-G. Unger, "Der Rechteckhohlleiter mit rechteckigem Stoffeinsatz," *Arch. Elek. Übertragung.*, vol. AEÜ-18, pp. 25–34, 1964.

[17] A. Lavik and H.-G. Unger, "Rückwärtswellen in homogenen Wellenleitern," *Arch. Elek. Übertragung.*, vol. AEÜ-18, pp. 35–42, 1964.

[18] A. S. Omar and K. Schünemann, "Space-domain decoupling of LSE and LSM fields in generalized planar guiding structures," *IEEE Trans. Microwave Theory Tech.*, vol. MTT-32, pp. 1626–1632, 1984.

[19] A. S. Omar and K. Shcünemann, "Generalized representation of Green's functions in multi-layer planar structures," in *Proc. 14th EuMC* (Liege), 1984, pp. 436–441.

[20] R. Mittra and S. W. Lee, *Analytical Techniques in the Theory of Guided Waves*. New York: Macmillan, 1971.

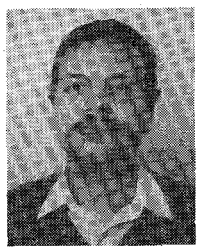

Abbas Sayed Omar was born in Sharkieh, Egypt, on December 9, 1954. He received the B.Sc. and M.Sc. degrees in electrical engineering from Ain Shams University, Cairo, Egypt, in 1978 and 1982, respectively.

From 1978 to 1982, he served as a Research and Teaching Assistant at the Department of Electronics and Computer Engineering of Ain Shams University, where he was engaged in investigations on microstriplines and below-cutoff waveguides and their use as a hybrid circuit technique for the realization of broad-band tunable oscillators. From 1982 to 1983, he joined the Institut für Hochfrequenztechnik, Technische Universität Braunschweig, Braunschweig, West Germany, as a Research Engineer, where he was involved with theoretical investigations on finlines. Since then he has held the same position at the Technische Universität Hamburg-Harburg, Hamburg, West Germany, where he is working towards the Doktor-Ing. degree. His current fields of research are the theoretical investigations of planar structures and dielectric resonators.

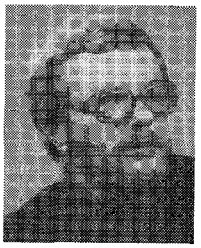

Klaus F. Schünemann (M'76) was born in Braunschweig, Germany, in 1939. He received the Dipl.-Ing. degree in electrical engineering and the Doktor-Ing. degree from Technische Universität Braunschweig, Germany, in 1965 and 1970, respectively.

Since 1983, he has been a Professor of Electrical Engineering and Director of the Arbeitsbereich Hochfrequenztechnik at the Technische Universität Hamburg-Harburg, Germany.

He has worked on nonlinear microwave circuits, diode modeling, solid-state oscillators, PCM communication systems, and integrated-circuit technologies such as finline and waveguides below cutoff. His current research interests are concerned with transport phenomena in submicron devices, CAD of planar millimeter-wave circuits, opto-electronics, and gyrotrons.